

Prediction of Silicon Direct Nitridation Kinetic by an Efficient and Simple Predictive Model Based on Group Method of Data Handling

E. Shahmohamadi, A. Mirhabibi^{1,*} and F. Golestanifard

* ar.mirhabibi50@gmail.com

Received: January 2019

Revised: July 2019

Accepted: September 2019

¹ School of Metallurgy and Materials Engineering, Iran University of Science and Technology (IUST), Tehran, Iran.

DOI: 10.22068/ijmse.16.4.77

Abstract: In the present study, a soft computing method namely the group method of data handling (GMDH) was applied to develop a new and efficient predictive model for prediction of conversion percentage of silicon. A comprehensive database was obtained from experimental studies in the literature. Several effective parameters like time, temperature, nitrogen percentage, pellet size, and silicon particle size were considered. The performance of the model was evaluated through statistical analysis. Moreover, the silicon nitridation was performed in 1573 K and the experimental results were evaluated against model results for validation of the model. Furthermore, the performance and efficiency of the GMDH model were confirmed against the two most common analytical models. The most effective parameters in estimating the conversion percentage were determined through sensitivity analysis based on the Gamma Test. Finally, the robustness of the developed model was verified through parametric analysis.

Keywords: Ceramics, Modeling, Silicon Nitriding, Programming, Kinetics, Pattern, Regression.

1. INTRODUCTION

Silicon nitride as one of the most practical engineering ceramics has been widely applied as a high-temperature structural material. Several advantages such as high resistance against thermal shock and corrosion, high strength, lower density in comparison with a metallic component, and biocompatibility make it popular as a structural material in cutting tools, gas turbine, diesel engine, precision bearings and biomedical applications [1–5]. Several methods such as hot-pressed silicon nitride (HP-SN), hot isostatic pressed silicon nitride (HIP-SN), sintered silicon nitride (SSN), gas partial sintered silicon nitride (GPS-SN), reaction bonded silicon nitride (RBSN), and sintered reaction bonded silicon (SRBSN) have been introduced for producing silicon nitride samples [6]. In this study, the RBSN method is investigated.

RBSN, which is also known as the direct nitridation of silicon, is one of the most economical methods to produce the silicon nitride for near net shape formation in comparison with the other methods. Although the RBSN method is cost-effective, it takes time to complete nitriding. In this method, Si_3N_4 is

formed by reacting of nitrogen and silicon at temperature between 1250 to 1400°C. For temperatures higher than 1400°C, reaction transfers into the liquid phase and consequently, different mechanisms are operative. Formation of silicon nitride occurs in three kinetic stages. In the first stage, kinetic of reaction is approximately zero because it takes time to initiate the nucleus of silicon nitride. At the second stage, nitridation is progressed by a reaction between silicon and nitrogen-based on different mechanisms of reactant diffusion in the inter-particle pores. It should be stated that the most progress in reaction occurs in this stage. At the final stage, diffusion paths into the core of particles are blocked by the reaction products; therefore, reaction gas should find a new path through reaction product to complete nitridation of silicon pellet. As a consequence, the kinetic of nitridation is decreased.

In the entire possible reaction temperature range (more than 1250 °C) [6], thermodynamics shows that the reaction is exothermic. Therefore, reaction progress is not limited thermodynamically. As the reaction progresses, both chemical reaction and sintering in silicon powder cause changes in particles microstructures. This circumstance changes pore

density and affects reaction kinetics. Effective diffusivity of the reaction gas is directly dependent on the tortuosity of silicon pellet. Therefore, the effective diffusivity of gas changes as the reaction progresses. Several parameters like physical properties of silicon pellet (e.g. size, density, pore size, and pore type) and gas properties (composition, flow rate, and pressure) can affect reactant diffusivity. A flexible model that can effectively consider all these parameters is one of the most important issues in simulation and prediction of silicon nitridation kinetic behavior.

Several efforts have been made to model the kinetics of reaction [7–15]. Most of these models have been developed to illustrate gas-solid reactions (without the presence of a catalyst) (e.g.[7], [16–19]). Models are classified into three main groups: pore model [17], particle-pellet model [19], and volume reaction model [16]. The sharp interface model (SIM) [7], [16] has been introduced as a specific condition for gas-solid reactions for the cases that the primary particles are solid and nonporous. The main idea behind this assumption is that the reaction occurs in the sharp interface of reacted and unreacted solids while the reaction takes place in the whole pellet in case of the porous particles. SIM conditions could be applied to both particle-pellet and pore models.

Several models have been developed based on SIM conditions in the last decades. In particular, Chang et al.[9] developed a model which was based on the diffusion-controlled system. They assumed that grains in the pellet are non-porous. They present a linear relationship between conversion percentage and time. Li et al. [8] also considered different parallel reaction mechanisms and used them to develop a predictive model for conversion percentage. Ku and Gregory [20] considered the effect of particles size variations in their mathematical model. On the other hand, the presence of H_2 and O_2 in the reactant gas makes the prediction of reaction kinetic more complicated. In this regard, Dervisbegovic and Riley [21] developed a two-zone model for the reaction of silicon powder compact in the nitrogen/hydrogen atmosphere.

In general, there are different mechanisms that control the kinetics of silicon nitridation during the reaction. Mechanisms involved in the initial stage can be also completely different from the final stage. Furthermore, in the special duration of the reaction,

several mechanisms may act in parallel. In this regard, the mentioned analytical models cannot consider all the complex mechanisms involved during the reaction. As a result, there are always remarkable scatter between experimental results and the predictions of mentioned models during the entire reaction or only on a segment of the reaction. On the other hand, several influencing parameters may have effect on the reaction kinetic which make approaching to an accurate solution too hard and time-taking. Tackling such problem, a soft computational method based on regression-based machine learning that can relate the input(s) to the target of the problem can be of great advantage while facing with this kind of case with considerable complexity and non-linearity.

In recent decades, machine learning approaches such as Artificial Neural Networks (ANNs) and ANFIS as the most common soft computing methods have been employed to overcome these limitations in material science (e.g.[22–25]). Results confirmed the superior performance of data mining-based approaches. However, the ANN and ANFIS models do not give enough insight into the generated models and are not as easy to use as the empirical formulas. Among the soft computing methods, the GMDH network is known as a self-organized method to model and discover the behavior of unknown or complicated systems based on given input-output data points (Ivakhnenko 1971 [26]; Ivakhnenko and Ivakhnenko 2000 [27]). The main objective of this study is to investigate the efficiency of the GMDH network for predicting the kinetics of silicon nitridation. The main advantage of GMDH method in comparison with methods like ANN is that the dependencies between input parameters and output parameter are represented in parametric form as an equation while these dependencies are hidden within neural network structures in ANN method. To develop a simple and efficient predictive model based on GMDH, a comprehensive database from literature containing 2186 experimental results is applied. The developed GMDH model related the conversion percentage of silicon to the time, temperature, nitrogen percentage, pellet size, and silicon particle size. The developed GMDH results are also compared with the two most common existing models through statistical error indicators. The relative importance of significant parameters dealing with conversion percentage is also investigated through sensitivity analysis. The

robustness of the proposed GMDH model is also verified through a parametric analysis.

2. METHODOLOGY

GMDH has been introduced as one of the effective machine learning methods to detect the nonlinear patterns latent in the database. It was first introduced by Ivakhnenko in 1971 [26]. The nonlinear relationship between input variables and response ones are presented as polynomial forms. In fact, the algorithm chooses the most proper quadratic polynomial term by selecting the best coefficients for considered polynomial terms based on two independent variables at each layer. The GMDH algorithm applies two sets of data, i.e. training and validation, to develop the model. The best outputs are obtained based on the best combinations of independent input variables. To achieve this, a complicated form of the Volterra functional series which is known as Volterra – Kolmogorow polynomial is applied to obtain the best correlation between the response value and the multi-input variables as follows:

$$y_i = a + \sum_{i=1}^{N_v} b_i x_i + \sum_{i=1}^{N_v} \sum_{j=1}^{N_v} c_{ij} x_i x_j + \dots + \sum_{i=1}^{N_v} \sum_{j=1}^{N_v} d_{ij\dots k} x_i x_j \dots x_k \quad (1)$$

Where, N_v is the number of independent variables. The matrix of Input data which consists of N_v independent variables and N response observations is presented in Eq. 2. The left matrix includes response observations and the right one holds N_v independent variables.

$$\begin{matrix} y_1 & x_{11} & x_{12} & \dots & x_{1N_v} \\ y_2 & x_{21} & x_{22} & \dots & x_{2N_v} \\ \vdots & \vdots & \vdots & \vdots & \vdots \end{matrix} = \quad (2)$$

The quadratic polynomial term for two independent variables is presented in Eq. 3. For N_v input variables, the $\binom{N_v}{2}$ quadratic terms can be developed as follows:

$$\hat{y}_i = a_0 + a_1 x_{ip} + a_2 x_{iq} + a_3 x_{ip} x_{jq} + a_4 x_{ip}^2 + a_5 x_{jq}^2$$

$$p, q \in \left\{ 1, 2, \dots, \binom{N_v}{2} \right\} \quad (3)$$

The regression method is used to obtain the coefficients of quadratic polynomial terms. To obtain the best fit between prediction and real output observed, the least-squares method is applied. The main objective of the GMDH method is to minimize the square of deviation between the actual outputs and predicted ones as:

$$\delta^2 = \sum_{i=1}^N [y_i - \hat{y}_i]^2 \quad (4)$$

In Eq. 4. \hat{y}_i is the predicted output.

3. MODEL DEVELOPMENT

In this study, a predictive model based on GMDH method is developed to estimate the conversion percentages of Si to Si_3N_4 in the following reaction:



To develop the model, a comprehensive database obtained from the experimental results of Chang et al. is used. The total database consists of 2186 data points. Several effective parameters including time, temperature, pellet size, nitrogen percent, and silicon particle size are considered as input variables. These parameters are known as the most important parameters which affect gas diffusivity. The reactions such as reaction. (5) are classified as a diffusion-controlled reaction, which their kinetics are dependent on reactant gas diffusivity. Therefore, the mentioned parameters are selected as predictive variables for the estimation of the conversion percentage. The ranges of input and output variables are presented in Table 1. The statistical index including minimum, maximum, average, and standard deviation are presented for each parameter. The selected ranges for input variables cover practical ranges which the reaction often occurs. In fact, to progress the reaction, special physical conditions can be reached by selecting the values of input variables in the mentioned ranges.

For more illustration, the histograms of input

Table 1. Influencing variables and statistic data

Parameter	Symbol	MIN	MAX	Average	Standard deviation
Time [min]	t	0.005	239.8	101.76	72.83
Temperature [°K]	T	1448	1648	1604.12	48.96
Pellet size [mm]	PeS	3	12	5.06	2.45
Nitrogen percent [%]	NP	10	100	85.77	22.51
Silicon particle size [μm]	SP	1	5	1.54	1.15
Conversion percent [%]	CP	0.117	36.4	15.97	9.08

and output variables for different ranges are shown in Fig. 1. It should be noted that the developed model is more reliable in ranges in which data points are more concentrated. In this study, a new parameter is introduced to consider the effect of silicon particle size. This parameter includes five ranges of particle size (PS=1 (particle size<38 μm), PS=2 (38 μm <particle size<45 μm), PS=3 (45 μm <particle size<53 μm), PS=4 (53 μm <particle size<63 μm), and PS=5 (particle size>63 μm)).

Overfitting is one of the most important problems which occurs during the training of the used machine learning methods. Benzhaf et al. (1998) introduced a new method in order to reduce overfitting problem and enhance the generalization capability of the developed model based on these methods. In this method, primary input data sets are randomly divided into train data and test data subsets. The training data is used to develop a new ba-

sic model while the test data is used to examine the performance of the developed model. To achieve the best and more generalized predictive model, the performances of the trained model should be the same for both training and testing datasets. To achieve a reliable prediction model several data groups are examined. To reach a reliable model, the maximum, minimum, mean and standard deviations of parameters should reach some stability in the training and testing data subsets. In this study, 2186 data points are used to develop the final model. Therefore, 80% of data (1749 data points) are taken for the training set and the remaining 20% of data (437 data points) used for testing data set.

After data divisions, the training data was applied to the GMDH algorithm and the following equations are derived from the learning step for estimation of conversion percentage as:

4. EXPERIMENTAL PROCEDURE

Layer 1 (Number of Neurons=4):

$$X_6 = -260 + 0.29T + 0.25t - 3.7 \times 10^{-5}tT - 8.1 \times 10^{-5}T^2 - 0.00044t^2 \quad (6a)$$

$$X_7 = -2.9 + 0.057NP + 0.11t + 0.00094tNP + 0.0002NP^2 - 0.00043t^2 \quad (6b)$$

$$X_8 = 0.47 + 4.2PS + 0.19t - 0.0038tPS - 0.81PS^2 - 0.00042t^2 \quad (6c)$$

$$X_9 = 3.7 - NP + 0.032T + 0.00073TNP + 9.1 \times 10^{-5}NP^2 - 2.1 \times 10^{-5}T^2 \quad (6d)$$

Layer 2 (Number of Neurons=3):

$$X_{11} = -1.7 + 0.55X_7 + 0.7X_6 + 0.081X_6X_7 - 0.043X_7^2 - 0.042X_6^2 \quad (6e)$$

$$X_{12} = -1.4 - 0.51X_9 + 0.33X_8 + 0.064X_8X_9 + 0.026X_9^2 - 0.0093X_8^2 \quad (6f)$$

$$X_{13} = -4.2 + 0.5X_9 + 0.42X_6 + 0.069X_6X_9 - 0.025X_9^2 - 0.017X_6^2 \quad (6g)$$

Layer 3 (Number of Neurons=2):

$$X_{16} = -0.83 + 0.89X_{13} + 0.31X_{12} + 0.061X_{12}X_{13} - 0.061X_{13}^2 - 0.0067X_{12}^2 \quad (6h)$$

$$X_{17} = -1.1 + 0.7X_{12} + 0.49X_{11} - 0.054X_{11}X_{12} + 0.038X_{12}^2 + 0.0088X_{11}^2 \quad (6i)$$

Layer 4 (Number of Neurons=1):

$$CP (\%) = -0.61 - 0.35X_{17} + 1.4X_{16} - 0.79X_{16}X_{17} + 0.38X_{17}^2 + 0.41X_{16}^2 \quad (6j)$$

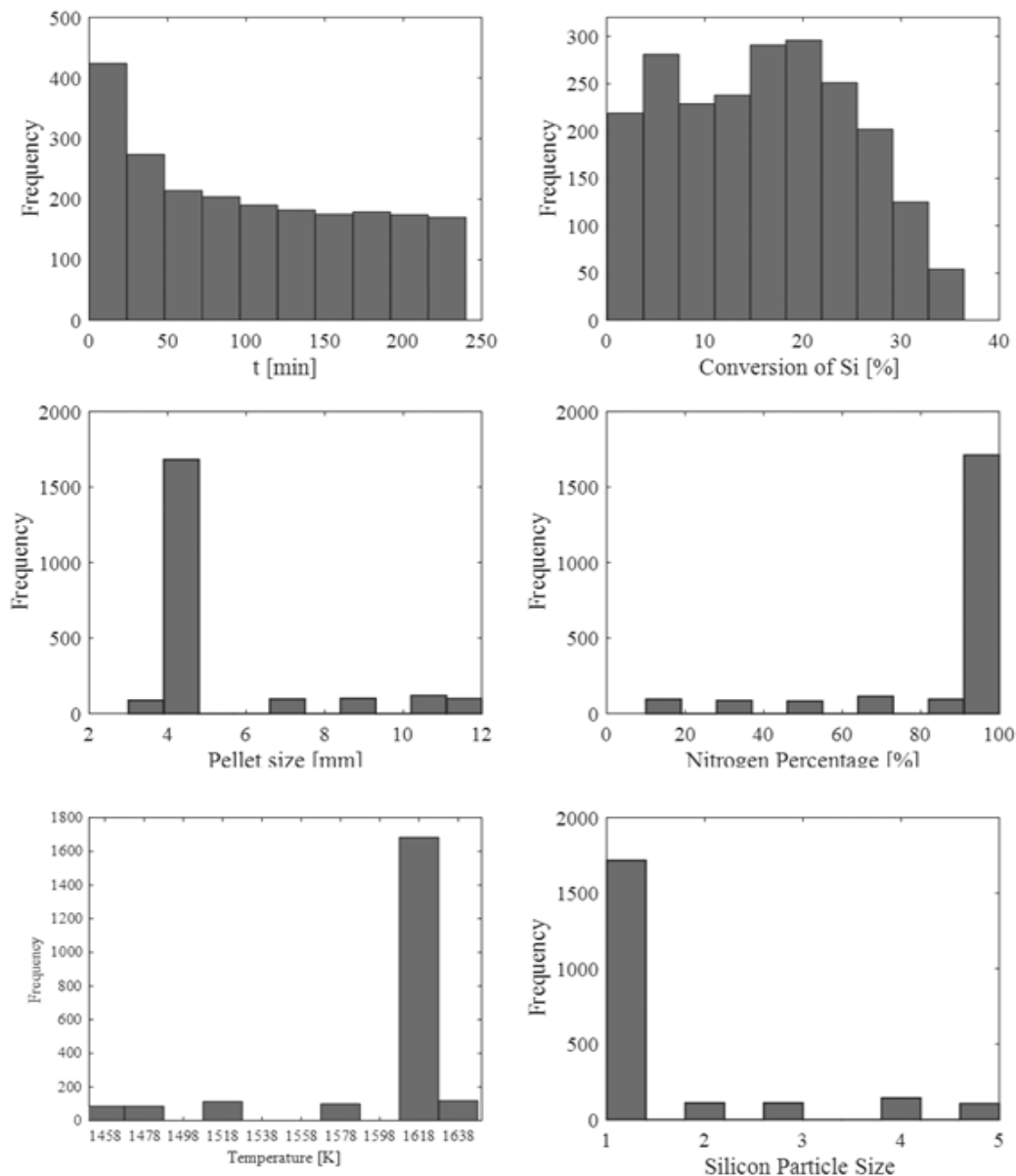


Fig. 1. Histograms of output and input variables

The material used for this research was 99.995% silicon powder ($D_{50} = 4.76 \mu\text{m}$, Dong-Fang Ref source, China) that was quantitatively characterized by spectrographic analysis before experimental tests. Other additional elements of the powder consisted of $<0.0001\%$ Ca and 0.0002% Mg. In addition, the particle size of silicon powder was measured by PSA (Particle Size Analyzer)(MAL100229, MALVEM) to set the initial conditions of the material. The green powder was compacted in stainless steel die at a pressure of 0.6 MPa to create a dense cylinder of

silicon shown in Fig.2. The compacted precursor was then cut into spherical pellets in order to minimize the touching distance between the sample and crucible.



Fig.2. compacted pure silicon after pressing

Taking the feedback of results of the prediction model into account, the completion time of the nitridation reaction was estimated and hence, 20 different time duration was chosen to calculate silicon nitridation percentage at 1573° k.

In order to perform the nitridation process of silicon, a tube electrical furnace was used. Since the oxygen decays the rate of nitridation by the unwanted formation of a thin layer of silicon dioxide, a small amount of hydrogen was purged into the nitrogen to remove the mentioned thin film. In this regard, 5 vol. % H₂ - 95vol. % N₂ composition was used as the reaction gas during the process. Pellet was accommodated in the tube furnace and held there for a specific time period while exposing to reaction gas at 1573°k. The procedure was carried out for 20 different time periods and reaction kinetics in terms of nitridation percentage was measured by pellet weight change and recording its increase after reaction completion.

4.1. Measuring of Nitridation Percentage

Due to the weight increase after reaction with nitrogen gas, the stoichiometric relations based on Equations (7) can be written to express this phenomenon as below. Also, experimental results are summarized in Table 2.



$$\Delta W = \text{Weight of } N_4 \text{ in } Si_3N_4 (g) \quad (8)$$

$$\frac{\Delta W}{2M_{N_2}} = mol_N = mol_{Si_3N_4} \quad (9)$$

$$\frac{\Delta W}{2M_{N_2}} .3 = mol_{Si} \quad (10)$$

$$\left(\frac{\Delta W}{2M_{N_2}} .3 \right) . M_{Si} = g_{Si} \quad (11)$$

$$X = \frac{3M_{Si} \Delta W}{2M_{N_2} W_0} \quad (12)$$

In abovementioned equations (7 - 12), X represents the reaction percentage, ΔW is the weight increase, W_0 is the pellet initial weight, M_{Si} is the molecular weight of silicon and M_{N_2} is the molecular weight of nitrogen

Table. 2. Experimental results

Time(min)	W ₀ (g)	Δ W(g)	X(%)
12	0.438	0.033	11.30137
25	0.304	0.031	15.29605
37	0.307	0.031	15.14658
50	0.208	0.022	15.86538
62	0.325	0.04	18.46154
75	0.371	0.045	18.19407
87	0.304	0.038	18.75
100	0.299	0.04	20.06689
112	0.271	0.036	19.9262
125	0.339	0.048	21.23894
137	0.382	0.052	20.41885
150	0.152	0.02	19.73684
162	0.134	0.02	22.38806
175	0.266	0.04	22.55639
187	0.31	0.045	21.77419
200	0.317	0.05	23.65931
212	0.338	0.054	23.9645
225	0.289	0.044	22.83737
237	0.315	0.05	23.80952
250	0.379	0.062	24.53826

5. RESULT AND DISCUSSIONS

In this study, the kinetics for the formation of Si₃N₄ was investigated using both experimental and soft computational approach and the results were compared to one another for verification of the proposed model. In addition, the validated model by experimental observations was compared with the work done by others and improved accuracy and superposition was seen for describing the kinetics of Si₃N₄ formation via reaction bonded method.

Results of XRD patterns and SEM micrographs demonstrate the extent of the reaction and morphology of formed phases. Furthermore, the performance of the developed model is evaluated through statistical error parameters. Then, the most important parameters in the estimation of conversion percentage are determined by using sensitivity analysis. To validate the model further,

the parametric analysis is done to ensure that the results of the developed model are in line with the physical concept latent in the problem.

5.1. Microstructure Analysis

The microstructure of nitrated pellet at 1573 °K after primary preparation was characterized by Scanning electron microscopy presented in Fig.3. Formation of α - Si_3N_4 is believed to have occurred through a vapor-liquid-solid (VLS) mechanism, or simply through a chemical vapor deposition (CVD) process between Si (g) and N_2 (g) reactants that could be considered as the dominant mode of nitride formation under flowing nitrogen condition. The presence of impurities may enhance the formation of α - Si_3N_4 . β - Si_3N_4 will also accompany the growth of the nitride layer. This will lead to the nitride forming through a gas-solid reaction in silicon surface due to diffusion of atomic nitrogen along β , or in the presence of liquid phase which may stimulate its production.

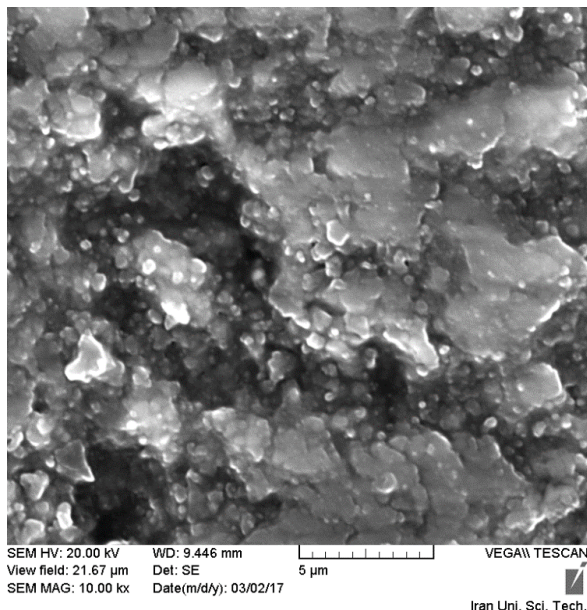


Fig.3. the microstructure of nitrated pellet at 1573°K

The x-ray diffraction pattern (Fig.4) of product reveals that the reacted silicon pellet contained unreacted silicon, and α - Si_3N_4 . There was no sign of silicon dioxide (SiO_2) and silicon oxynitride ($\text{Si}_2\text{N}_2\text{O}$) peaks in the pattern and the proportion of α - Si_3N_4 was much higher than that of β - Si_3N_4 . As can be seen in Fig.4, with the progress in the

reaction, there was a decrease in the intensity of Si peaks which was accompanied with an increase in the intensities of both α and β phases.



Fig. 4. XRD pattern of three pellets which nitrated for a)250, b)100, c)25 min.

5.2. Performance Analysis

To evaluate the performance of the developed GMDH model, four statistical error parameters including bias, root mean square error (RMSE), correlation coefficient (R) and coefficient of determination (R^2) are applied. The equations for these parameters are as follows:

$$\text{Bias} = \frac{\sum_{i=1}^N (P_i - O_i)}{N} \quad (13)$$

$$\text{RMSE} = \sqrt{\frac{1}{N} \sum_{i=1}^N (P_i - O_i)^2} \quad (14)$$

$$R = \frac{\sum_{i=1}^N (P_i - P_m)(O_i - O_m)}{\sqrt{(P_i - P_m)^2} \sqrt{(O_i - O_m)^2}} \quad (15)$$

$$R^2 = 1 - \frac{\sum_{i=1}^N (O_i - P_i)^2}{\sum_{i=1}^N (O_i - O_m)^2} \quad (16)$$

where, O_i is the measured value, P_i stands for prediction values; N is the number of data points, O_m is the mean value for observation and P_m is the mean value of prediction.

The results of the developed GMDH model and the actual experimental observations for training and testing datasets are depicted in Figs. 5 (a) and (b), respectively. Furthermore, the errors and the best fitted normal distribution on these errors are also shown in these figures. As shown, there are good agreement between the predicted conversion percentage by GMDH model and the observed data for both training and testing datasets. This indicates that the generalization capability of the developed model for unseen data points in the range of training dataset is acceptable. On the other hand, the errors of a good predictive model should follow a certain trend and distribution [28]. This feature can be useful for considering uncertainty in a predictive or design model. As indicated in Figs. 5 (a) and (b), the errors of the developed GMDH model approximately follow a normal distribution for both training and testing datasets. Therefore, the uncertainty of the GMDH model can be easily calculated by considering a random parameter with a normal distribution. As it was mentioned previously, four statistical error parameters such as *Bias*, *RMSE*, *R*, and R^2 are used.

To quantitatively evaluate the performance of the developed model, the statistical error parameters are presented in Table 3 for both training and testing datasets. In fact, the *R* parameter indicates the correlation between predicted and measured values. If the *R*-value is more than 0.8, it shows that there is a strong correlation between observed and predicted values. However, *R* sometimes may not necessarily indicate better model performance due to the tendency of the model to deviate towards higher or lower values, particularly when the data range is very wide and most of the data are distributed about their mean values. Therefore, in this study, the coefficient of determination, R^2 , is used because it can give the unbiased estimate and maybe a better measure for model performance. In addition, *Bias* and *RMSE* parameters should be close to zero for having accurate results.

According to Table 3, the GMDH model has the same performance for both training and testing

datasets. The *Bias* and *RMSE* values are the same and close to zero. It should be noted that *Bias* values for training and testing datasets are -0.01 and -0.11, respectively. This indicates that the GMDH model slightly underestimates the conversion percentage which makes the model conservative in the estimation of this parameter. The GMDH model, respectively, with $R=0.966$ and $R=0.965$ for training and testing datasets, satisfies the criterion for the strong correlation between predicted and observed outputs ($R > 0.8$) [29]. In addition, the R^2 values are also close to 1 and have acceptable values for both training and testing datasets.

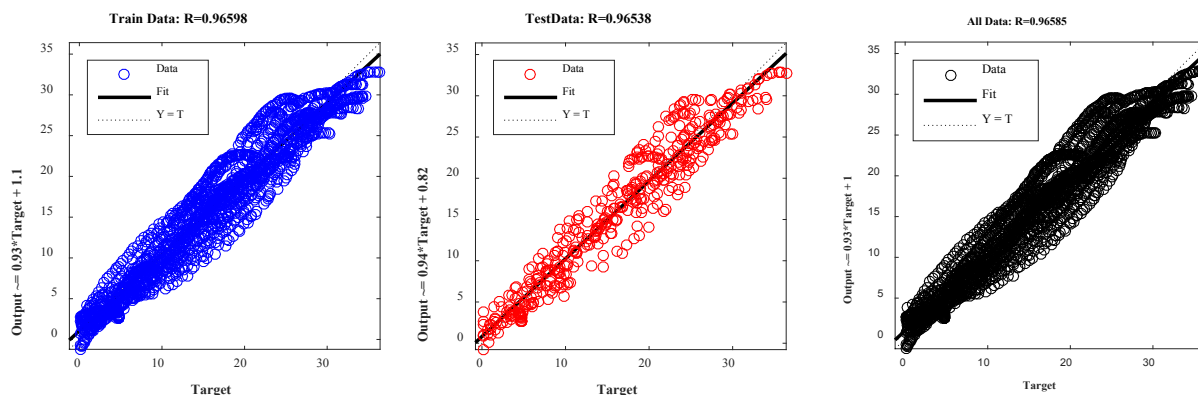
To schematically illustrate the correlation between observed and predicted outputs, comparisons between experimental results and model prediction for testing, training, and the whole datasets are shown in Fig. 5. In this figure, the best linear regression lines between real and predicted output are also shown. It is clear from this figure that the fitted linear equations are nearly the same as the optimal line of $y=x$. In general, the results



Fig. 5. Results of predicted model and experimental observations a)train, b)test

Table 3. Validation of the proposed model by Statistical error measures

Item	Formula	Condition	Training data set	Testing data set
<i>BIAS</i>	$Bias = \frac{\sum_{i=1}^N (P_i - O_i)}{N}$	$ BIAS \rightarrow 0$	-0.0172	-0.1161
<i>RMSE</i>	$RMSE = \sqrt{\frac{1}{N} \sum_{i=1}^N (P_i - O_i)^2}$	$RMSE_{train} = RMSE_{test}$	2.3458	2.3827
<i>R</i>	$R = \frac{\sum_{i=1}^N (P_i - P_m)(O_i - O_m)}{\sqrt{(P_i - P_m)^2} \sqrt{(O_i - O_m)^2}}$	$R > 0.8$	0.9660	0.9654
R^2	$R^2 = 1 - \frac{\sum_{i=1}^N (O_i - P_i)^2}{\sum_{i=1}^N (O_i - O_m)^2}$	$R^2 \rightarrow 1$	0.9331	0.9317

**Fig. 6.** Comparison between predicted outputs and experimental results

indicates that the developed model has a reliable and sufficient predictive ability. The model has to get the ability to get general knowledge from a set of data by synchronization of weights and bias which is called training. In the case of over fitting, the network memorizes some local rules instead of realistic pattern recognition which yields unwanted chaos in testing phase and finally, indecent modeling.

To further evaluate the performance of the developed GMDH model, its prediction is compared with two common previous models put forward by Li et al. (1997) and Chang et al. (2000). Li et al. (1997) and Chang et al. (2000) are two well-known general models for the prediction of kinetics of silicon direct nitridation and several effective parameters and mechanisms that control the reaction progress are included in their models. Therefore, the mentioned models can be applied as reliable references to evaluate the developed

GMDH model. To compare the performances of the models, temperature and nitrogen percentage are selected as 1573°k and 95%, respectively. These values for temperature and gas concentration are the most common reaction conditions which are often used to ensure the occurrence of the reaction. Based on comparison performed between the results of two mentioned models, a cross-validation graph was developed using established GMDH model and real experimental data (Fig. 7). As shown, both models of Li et al. (1997) and Chang et al. (2000) perform well at initial times of reaction and their predictions are in agreement with experimental results. However, their predictions are remarkably overestimated after the time of 75 min. According to this figure, in general, the developed GMDH model showed a remarkable agreement with experimental results for the whole duration of reaction and outperformed the other models.

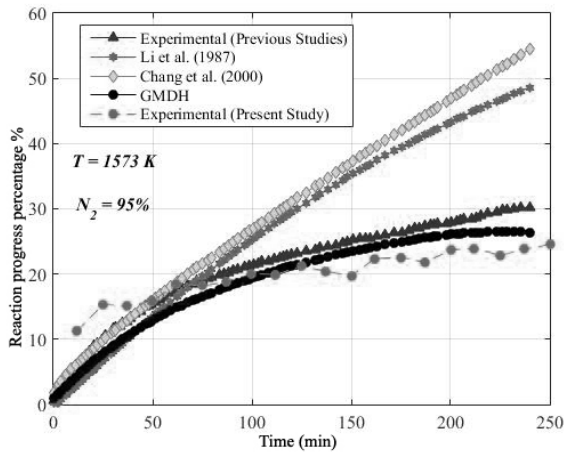


Fig. 7. comparisons between the results of Li et al. (1997) and Chang et al. (2000) and the developed GMDH models

5.3. Sensitivity Analysis

To determine the most important parameters in the estimation of conversion percentage, a sensitivity analysis (ST) was performed. To achieve this, the Gamma Test (GT) is applied. GT is a way to show the degree of an input efficacy on the model outputs. It is often done in a model which is multivariable. In general, selecting the best combination of input variables is one of the most important concerns in the modeling process of intelligent approaches such as GMDH [30]. To illustrate the GT analysis more, suppose the following set as:

$$\{(x_i, y_i), 1 \leq i \leq M\} \quad (12)$$

Where, $x \in R^m$ is the input vector (m is the number of input variables), $y \in R$ is the output vector, and M represents the number of observations recorded in the experimental study. In GT analysis, the relationship between input and output variables by considering uncertainty and errors involved in the modeling process can be stated as:

$$y = f(x_1, x_2, \dots, x_m) + r \quad (13)$$

Where, f is a smooth function and r is a noise variable with a random nature. In the first step, the GT calculates the k th nearest neighbor distances for each X_i vector ($N[i, k]$). Then, the mean square distance to the k th nearest neighbor ($\delta_M(k)$) and

the corresponding gamma function of the output variable ($\gamma_M(k)$) are calculated as follows:

$$\delta_M(k) = \frac{1}{M} \sum_{i=1}^M |x_{N(i,k)} - x_i|^2 \quad 1 \leq k \leq p \quad (18)$$

$$\gamma_M(k) = \frac{1}{2M} \sum_{i=1}^M |y_{N(i,k)} - y_i|^2 \quad 1 \leq k \leq p \quad (19)$$

where, p is the nearest neighbors. At the final step, the relationship between input and output variables is estimated based on a linear regression equation as follows:

$$\gamma = A\delta + \Gamma \quad (20)$$

$$V_{ratio} = \frac{\Gamma}{\sigma^2(y)} \quad (21)$$

In Eq. (20), the y-intercept represents the value of gamma and the Gamma value close to zero indicates that the performance of the model is better. The gradient of the mentioned linear equation represents the complexity of the model (the steeper slope, the more complex model). In Eq. (21), $\sigma^2(y)$ is the variance of the output variable (y) and V_{ratio} is a parameter that varies between zero and 1. The value of V_{ratio} close to zero indicates that there is a high degree of accuracy in the prediction of output variables by the developed model.

To obtain the order of importance and effectiveness of considered input parameters, six scenarios are considered. In the first scenario, all input parameters are used in the GT analysis. In the next scenarios, all input parameters are excluded one by one from the GT analysis. The variations in gamma parameters such as V_{ratio} are calculated after removing each parameter. The more variations V_{ratio} indicate the more important of the removed parameter in the estimation of the conversion percentage. In fact, the value V_{ratio} indicates the deviation of predictions from the observed outputs.

Results of GT analysis are summarized in Table 4. To better illustrate the results of GT analysis, the values of V_{ratio} different scenarios are shown in Fig. 8. According to Table 4, time, nitrogen percentage, and reaction temperature are the most effective parameters in the estimation of conversion percentage. In fact, these results are also in agreement with the physics of the reaction. In general, silicon nitride is formed in two phases of α -Si₃N₄ and β -Si₃N₄ [31]. Forma-

tion of two phases happens in separate diffusional mechanisms, which are slow and can be affected by different variables. Therefore, reaction time plays an important role which gives a chance to reactants to diffuse through product shell around the particle. Furthermore, the results of Chang et al. (2000), Li et al. (1997), and experimental data indicate that reaction time is directly related to reaction progress. Therefore, the GT analysis has accurately determined the time parameter as the most important parameter.



Fig. 8. Results of Gamma Test (the values of V_{ratio} for different scenarios)

The GT analysis also detected the nitrogen percentage as the second important parameter. In fact, the density of silicon nitride nuclei on the reaction interface depends on the amount of adsorbed nitrogen (or silicon). The amount of adsorbed nitrogen is also affected by nitrogen pressure at the reaction interface. As the pressure increases, the amount of adsorbed nitrogen increases at the interface. Higher pressures form more primary Si_3N_4 nuclei and increase the initial kinetic. Furthermore, high pressure makes diffu-

sion mechanisms faster by increasing the concentration of nitrogen in the inter-particle pores.

Diffusion, which plays as a controlling parameter in the rate determination of some reactions, is also very sensitive to the temperature. The mobility of diffuse reactant highly depends on the temperature variable because of its high activation energy. Previous studies [8–10], [14], [32], [33] indicated that diffusion of nitrogen through the product shell is possible only if nitrogen decomposes into the atomic state. If there is no oxygen, hot surfaces are the only sources for producing the atomic nitrogen. Since nitrogen dissociation requires a lot of energy, diffusion is strongly dependent on the temperature. Another words, it is possible that the reaction takes place in the vapor state. It means that the silicon vapor reacts with nitrogen. In the vapor state reaction, the temperature has the main role in producing enough silicon vapor pressure. In general, the results of GT analysis are in line with previous findings in the literature.

5. 4. Parametric Analysis

To better validate the robustness of the developed model, a parametric analysis is performed to ensure that the results of the proposed GMDH model are in line with physical concepts of the reaction kinetics. The methodology of parametric analysis is based on the variation of the model results with changing in one variable while other variables are kept at their average values. As stated in the previous section, time, nitrogen percentage, and temperature were the most important parameters. Therefore, the effect of these parameters were investigated more by applying the paramet-

Table 4. Results of Gamma Test analysis

Scenarios	Unconsidered variable	Gamma	Gradient	Standard Error	V-ratio
1	Nothing (all inputs are considered)	-4.45E-5	0.5853	6.6159E-5	-0.000178
2	Time	0.2250	0.0305	0.02945	0.90023
3	Temperature	0.0339	-0.4474	0.00172	0.1356
4	Pellet size	0.0079	0.3513	0.000706	0.03163
5	Nitrogen percentage	0.0682	-1.4864	0.00522	0.2731
6	Silicon particle size	0.01368	0.1730	0.0009	0.0547

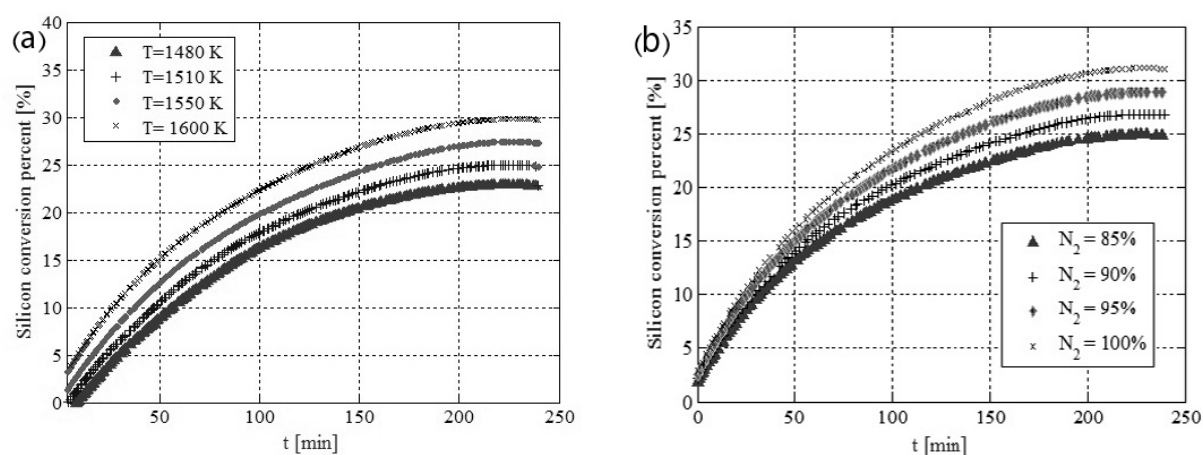


Fig. 9. The results of the parametric analysis for a) different temperatures b) nitrogen percentage

ric analysis. The results of the parametric analysis are presented in Fig. 9. The variation of silicon conversion percentage with reaction duration for four different temperatures ($T=1480$, 1510 , 1550 and 1600 C) and four different nitrogen percentage ($N_2=85$, 90 , 95 and 100%) are shown in Fig. 9 (a) and (b), respectively. As shown in this fig., the conversion percentage increases as the temperature and nitrogen percentage increase and also the increasing effects of temperature and nitrogen percentage on conversion percentage increase with the progress in the reaction. The increase of conversion percentage with temperature and nitrogen percentage is due to the fact that the silicon nitridation is generally controlled by nitrogen diffusion, which it is also highly dependent on the reaction temperature and reactant concentration. Furthermore, at the initial time of reaction, silicon is directly exposed to reactant gas while the product shell seals the whole side of the pellet as the reaction progresses, and consequently, the diffusion of reactants could be more important. As a result, temperature and nitrogen percentage parameters which can be also have an effect on reactant diffusion show more influence on conversion percentage at later times in comparison with initial stages. In general, it can be concluded from this figure that the developed GMDH model correctly captured these physical patterns. It should be noted that the variations of silicon conversion percentage are more influenced by the nitrogen percentage in comparison with temperature parameter. Similar observation is also reported in

sensitivity analysis and previous studies [8]–[10], [13]–[15], [20], [32], [33].

6. CONCLUSIONS

In the present study, an effective predictive model based on the group method of data handling (GMDH) is developed to estimate the kinetics of silicon nitride formation. Based on the results, obtained the following remarks can be highlighted:

1. The dependency of involved parameters upon conversion percentage such as time, temperature, nitrogen percentage, pellet size, and silicon particle size was studied using the proposed model.
2. The accuracy of the developed GMDH model was evaluated through statistical error parameters and results of performance analysis indicated that model efficiency with $R^2=0.93$ as a remarkable estimation approach of conversion percentage.
3. The kinetics of the reaction was expressed in terms of reaction rate at 1573 K and results were compared with two models of Chan (2000), Li (1997) and data of experimental measurement. Results showed that the previous models perform well in initial times of reaction while their predictions are remarkably overestimated after the time of 75 min . In summary, GMDH model showed superior predictability for the whole duration of the reaction.
4. In order to establish a sensitivity analysis

for prediction of conversion percentage, the Gamma Test (GT) is applied and it indicated that the time and nitrogen percentage are the most significant parameters. While temperature, silicon particle size, and pellet size are other less important parameters.

5. To verify the results of the developed and its accordance with physical concepts latent in the problem, the parametric analysis was also implemented which confirmed the robustness of the GMDH model in the development of physical patterns both in the present and the previous studies.

REFERENCES

1. Yigiterol, F., Güllü, H. H., Bayraklı, Ö., Yıldız, D. E., "Temperature-Dependent Electrical Characteristics of Au/Si₃N₄/4H n-SiC MIS Diode," *J. Electron. Mater.*, 2018, 47, 5, 2979–2987.
2. Vieira, E. M. F., Ribeiro, J. F., Sousa, R., Silva, M. M., Dupont, L., Gonçalves, L. M., "Titanium Oxide Adhesion Layer for High Temperature Annealed Si/Si₃N₄/TiO_x/Pt/LiCoO₂ Battery Structures," *J. Electron. Mater.*, 2016, 45, 2, 910–916.
3. Torchynska, T., Khomenkova, L., Slaoui, A., "Modification of Light Emission in Si-Rich Silicon Nitride Films Versus Stoichiometry and Excitation Light Energy," *J. Electron. Mater.*, 2018, 47, 7, 3927–3933.
4. Lu, Y., Yang, J., Lu, W., Liu, R., Qiao, G., Bao, C., "Synthesis of Porous Silicon Nitride Ceramics from Diatomite," *Mater. Manuf. Process.*, 2010, 25, 9, 998–1000.
5. Zhang, X. H., Chen, G. Y., An, W. K., Deng, Z. H., Liu, W., Yang, C., "Experimental Study of Machining Characteristics in Laser Induced Wet Grinding Silicon Nitride," *Mater. Manuf. Process.*, 2014, 29, 11–12, 1477–1482.
6. Somiya, S., Mitomo, M., Yoshimura, M., "SILICON NITRIDE - Ceramic Research and Development in Japan," *Mater. Manuf. Process.*, 1991, 6, 4, 741–744.
7. Carter, R. E., "Kinetic Model for Solid-State Reactions," *J. Chem. Phys.*, 1961, 34, 6, 2010–2015.
8. Li, W. B., Lei, B. Q., Lindbäck, T., "A kinetic model for reaction bonding process of silicon powder compact," *J. Eur. Ceram. Soc.*, 1997, 17, 9, 1119–1131.
9. Chang, F.-W., Liou, T. H., Tsai, F. M., "The nitridation kinetics of silicon powder compacts," *Thermochim. Acta*, 2000, 354, 1–2, 71–80.
10. Wang, X. S., Zhai, G., Yang, J., Wang, L., Hu, Y. and et al., "Nitridation of Si(111)," *Surf. Sci.*, 2001, 494, 2, 83–94.
11. Hara, Y., Shimizu, T., Shingubara, S., "Nitridation of silicon by nitrogen neutral beam," *Appl. Surf. Sci.*, 2016, 363, 555–559.
12. Hyuga, H., Zhou, Y., Kusano, D., Hiroa, K., Kita, H., "Nitridation behaviors of silicon powder doped with various rare earth oxides," *J. Ceram. Soc. Japan*, 2011, 119, 1387, 251–253.
13. Li, Y. et al., "Study on Nitridation of Silicon Added With Amorphous Silicon Nitride," *Proceeding of Nano and Micro Materials, Devices and Systems; Microsystems Integration*. ASME, New York, USA, 2011, 435–438.
14. Zhu, X., Zhou, Y., Hirao, K., Lenčič, Z., "Processing and Thermal Conductivity of Sintered Reaction-Bonded Silicon Nitride. I: Effect of Si Powder Characteristics," *J. Am. Ceram. Soc.*, 2006, 89, 11, 3331–3339.
15. Kim, M., Park, J., Lee, H.-W., Kang, S., "A cyclic process for the nitridation of Si powder," *Mater. Sci. Eng. A*, 2005, 408, 1–2, 85–91.
16. Ishida, M., Wen, C. Y., "Comparison of zone-reaction model and unreacted-core shrinking model in solid–gas reactions—I isothermal analysis," *Chem. Eng. Sci.*, 1971, 26, 7, 1031–1041.
17. Bhatia, S. K., "Analysis of distributed pore closure in gas-solid reactions," *AIChE J.*, 1985, 31, 4, 642–648.
18. Ishida, M., Wen, C. Y., Shirai, T., "Comparison of zone-reaction model and unreacted-core shrinking model in solid–gas reactions—II non-isothermal analysis," *Chem. Eng. Sci.*, 1971, 26, 7, 1043–1048.
19. Szekely, J., Evans, J. W., "A structural model for gas–solid reactions with a moving boundary," *Chem. Eng. Sci.*, 1970, 25, 6, 1091–1107.
20. Ku, W., Gregory, O. J., Jennings, H. M., "Computer Simulation of the Microstructure Developed in Reaction-Sintered Silicon Nitride Ceramics," *J. Am. Ceram. Soc.*, 1990, 73, 2, 286–296.
21. Dervisebegovic, H., Riley, F. L., "The influence of iron and hydrogen in the nitridation of silicon," *J. Mater. Sci.*, 1979, 14, 5, 1265–1268.
22. Maleki, E., Maleki, N., "Artificial Neural Network Modeling of Pt/C Cathode Degradation in PEM Fuel Cells," *J. Electron. Mater.*, 2016, 45, 8, 3822–3834.
23. Vafaeezad, H., Seyedein, S. H., Aboutalebi, M. R., Eivani, A. R., "Incorporating the Johnson–Cook Constitutive Model and a Soft Computational Approach for Predicting the High-Temperature Flow Behavior of Sn-5Sb Solder Alloy: A Comparative Study for Processing Map Develop-

- ment,” *J. Electron. Mater.*, 2017, 46, 1, 467–477.
24. Derebasi, N., Eltez, M., Guldiken, F., Sever, A., Kallis, K., Kilic, H., “Influence of Geometrical Factors on Performance of Thermoelectric Material Using Numerical Methods,” *J. Electron. Mater.*, 2015, 44, 6, 2068–2073.
25. Reddy, N. S., Panigrahi, B. B., Ho, C. M., Kim, J. H., Lee, C. S., “Artificial neural network modeling on the relative importance of alloying elements and heat treatment temperature to the stability of α and β phase in titanium alloys,” *Comput. Mater. Sci.*, 2015, 107, 175–183.
26. Ivakhnenko, A. G., “Polynomial Theory of Complex Systems,” *IEEE Trans. Syst. Man. Cybern.*, 1971, 4, 364–378.
27. Ivakhnenko, A. G. Ivakhnenko, G. A., “Problems of further development of the group method of data handling algorithms. Part I,” *PATTERN Recognit. IMAGE Anal.*, 2000, 10, 2, 187–194.
28. Kaveh, A., Bakhshpoori, T., Hamze-Ziabari, S. M., “Derivation of New Equations for Prediction of Principal Ground-Motion Parameters using M5' Algorithm,” *J. Earthq. Eng.*, 2016, 20, 6, 910–930.
29. Smith, G. N., *Probability and statistics in civil engineering*. Collins, London., UK, 1986, 158-186.
30. Kaveh, A., Hamze-Ziabari, S. M., Bakhshpoori, T., “Patient rule-induction method for liquefaction potential assessment based on CPT data,” *Bull. Eng. Geol. Environ.*, 2018, 77, 2, 849–865.
31. Karakuş, N., Kurt, A. O., Toplan, H. Ö., “Production of Sinterable Si_3N_4 from $\text{SiO}_2\text{-Li}_2\text{O-Y}_2\text{O}_3$ Mixture,” *Mater. Manuf. Process.*, 2012, 27, 7, 797–801.
32. Pigeon, R. G., Varma, A., “Quantitative kinetic analysis of silicon nitridation,” *J. Mater. Sci.*, 1993, 28, 11, 2999–3013.
33. Hughes, G. S., Mcgreavy, C., Merkin, J. H., “Transport effects in the manufacture of reaction-bonded silicon nitride,” *Can. J. Chem. Eng.*, 1979, 57, 2, 198–202.